



Origin of Changbaishan volcano inferred from simulation of the Cenozoic Pacific plate subduction using geodynamic models with data assimilation

Tao Zhu^{1,2}, Yingxing Guo^{1,2}, Yueyang Xia^{1,2}, Chao Dong^{1,2}

5 ¹Institute of Geophysics, China Earthquake Administration, Beijing 100081, China

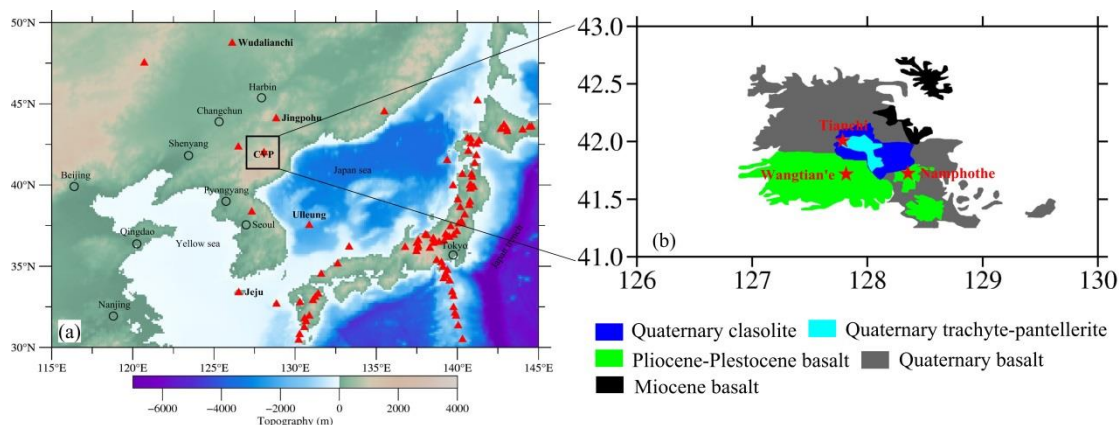
²Beijing Baijiatuan Earth Sciences National Observation and Research Station, Beijing 100095, China

Correspondence to: Tao Zhu (ZXL_TAO@126.COM)

Abstract. The Changbaishan volcano has been considered a giant active intraplate volcano with hidden potentially disastrous eruptive risks, so its origin has attracted widespread attention from all over the world. However, this issue has not
10 been adequately settled down due to its complexity. So far, three primary conceptual mechanisms have been proposed based on seismic tomography and geochemistry. All three mechanisms have been considered to be correlated with the subduction of the Pacific plate. Therefore, we use the best-fit thermochemical geodynamic model with data assimilation, which was determined by tracking the seismically inferred structure of the subducted Pacific slab beneath the Changbaishan volcanic province (CVP), to assess the their relative significance. The findings suggest that the super-hydrous melts in the mantle atop
15 the Pacific slab, resulting from the slab dehydration in the mantle transition zone (MTZ), may primarily contribute to the volcanism of the Changbaishan volcano. Meanwhile, the other two mechanisms, the upward escape of the entrained oceanic asthenospheric material as well as the piling up and thickening of the subducted Pacific slab, may play secondary roles.

1 Introduction

The Changbaishan volcano, located in the border area between China and North Korea (Fig. 1a), is a giant Cenozoic
20 intraplate active stratovolcano in Northeast Asia, featuring three main craters of Tianchi spanning China and DPR Korea, Wangtian'e in China, and Namphothe in DPR Korea (Fig. 1b). The volcano has erupted massively many times since the Miocene and has been under unrest in the last 20 years, so it has the risk of potentially disastrous eruption (Acocella et al., 2015; Wei et al., 2013; Xu et al., 2012; Wu et al., 2007; Hong et al., 2007). The formation mechanism of the Changbaishan volcano is complex and has been under debate so far, and there is still no final conclusion. The following conceptual models
25 are proposed. First, the Changbaishan volcano is considered to be a hotspot volcano related to a mantle plume, similar to the Hawaiian volcano (Lv et al., 2007; Wang et al., 1999). This mechanism is supported by the results of the receiver function (He et al., 2014, 2016), but more seismic tomography results do not support the existence of a mantle plume beneath the CVP (e.g., Guo et al., 2016, 2018; Wei et al., 2015; Zhao et al., 2009; Chen and Pei, 2010; Huang and Zhao, 2006; Lei and Zhao, 2005). Consequently, it is ruled out (Tang et al., 2014). The second mechanism is asthenospheric injection proposed



30

Figure 1: (a) Location of the Changbaishi volcanic province (CVP) and (b) the magma distribution of the Changbaishan volcano with ages. Red triangles stand for volcanoes.

by Tatsumi et al. (1990). This mechanism does not take into account the role of the stagnant Pacific slab within the MTZ.

35 Seismic tomography results have revealed that the Pacific plate has subducted beneath the CVP and is stagnant within the MTZ, with the mantle and lithosphere above it exhibiting lower seismic wave velocities (Takeuchi et al., 2014; Lei et al., 2013; Zhao et al., 2009; Lei and Zhao, 2005). This may be caused by the dehydration of the subducted plate at deep mantle, which leads to the decompression melting of mantle rocks (Sheng et al., 2016; Thybo and Perchuc, 1997). Consequently, some investigators have refined this mechanism and proposed a model of the upwelling of hot and wet asthenospheric

40 materials. This upwelling is jointly driven by mantle convection within the big mantle wedge and the dehydration of the stagnant subducted Pacific slab within the MTZ beneath the CVP (Du and Lei, 2019; Chen et al., 2017; Zhao et al., 2009, 2017; Tian et al., 2016; Wei et al., 2015; Lei et al., 2013; Zhao and Liu, 2010; Tang et al., 2006; Huang and Zhao, 2006; Lei and Zhao, 2005). This mechanism has been questioned by geochemical findings that the volcanics collected from the Changbaishan volcanic province exhibited excess ^{230}Th (Zou et al., 2008, 2010) and non-negative Nb and Ta anomalies

45 (Chen et al., 2007), indicating that the subducting Pacific plate does not contribute materially to the volcanics (Fan and Zhang, 2012; Zou et al., 2008). Accordingly, an alternative mechanism is proposed, in which the upwelling and decompression melting of asthenospheric material occur due to big mantle wedge convection and the piling up and thickening of the subducted Pacific slab within the MTZ (Zou et al., 2008). However, some researchers hold opposing views on the issue of material contribution from the subducting Pacific plate (e.g., Choi et al., 2017; Ma et al., 2015; Wang et al.,

50 2000). Thirdly, recent seismic tomography results have revealed gaps between the segments of the stagnant Pacific slab within the MTZ. These gaps are filled with notably low-velocity materials extending upwards to a depth of ~60 km (Guo et al., 2018). Therefore, some researchers suggested that the subducting Pacific plate entrains enormously its underlying asthenospheric material into the MTZ, and that the Changbaishan volcano was the result of upwelling caused by the upward escape of these entrained asthenospheric material through the gaps between the slab segments (Guo et al., 2016, 2018; Liu



55 and Zhou, 2015; Tang et al., 2014). Fourthly, some researchers considered that the formation of the Changbaishan volcano was related to the rollback of the subducting Pacific plate and the convection in the big mantle wedge above the stagnant slab (Guo et al., 2015; Wei et al., 2012). However, this mechanism is unlikely to generate magma that could sustain the long-term volcanic activity of the Changbaishan volcano (Strak and Schellart, 2014). Among the proposed conceptual mechanisms of the Changbaishan volcano, there are three most likely possibilities. These include upwellings caused by the
60 dehydration, and the piling up and thickening of the stagnant Pacific slab within the MTZ, as well as the upward escape of the entrained asthenospheric material from the MTZ through gaps between the slab segments. However, which of these mechanisms is both reasonable and irreplaceable? Determining this solution may necessitate the consideration of additional methods.

Geodynamic modeling is a commonly used and effective method to study the origin of a volcano. Specifically, regarding
65 the mantle plume mechanism, Leonard and Liu (2016) studied its role and effect on the volcanic activity of Yellowstone by utilizing a four-dimensional mantle convection model based on the subduction history of the Farallon Plate. The results showed that the mantle plume was not the main cause. Regarding the dehydration mechanism of subducting plates, the thermo-mechanical simulations (Sheng et al., 2016; Li et al., 2019) indicate that a small amount of water can be retained within subducting plates and transported to the MTZ. The amount of water dehydrated from the subducting plates at deep
70 mantle is the primary factor influencing the magma volume and eruptive intensity of the Changbaishan volcano. Regarding the slab sinking mechanism, studies have shown that volcanic activity above or near the front end of a stagnant slab may be related to the upwelling flow accompanying slab sinking (Kameyama and Nishioka, 2012). Regarding the mechanism of the piling up and thickening of subducting slabs, Motoki and Ballmer (2015) points out that the subducting slabs trapped within the MTZ inherently possess convective instability. Weak plates can become unstable within tens of millions of years,
75 generating upwelling from the lower part of the stagnant slabs, which are then entrained by surrounding mantle flows to the base of the lithosphere, triggering decompression melting. Furthermore, the convective instability of slabs can segregate the slab compositions, with harzburgite components ascending into the upper mantle while eclogite components sinking into the lower mantle. This segregation process can sustain the compositional gradient between the upper and lower parts of the MTZ over millions of years. Regarding the mechanism of the upward escape of entrained asthenospheric material, studies have
80 shown that asthenospheric material underlying a subducting slab can be entrained into the MTZ, even into the lower mantle (Liu and Zhou, 2015; Faccenda and Capitanio, 2013). This material may intermittently escape upwards through gaps between slab segments, resulting in upwelling (Liu and Zhou, 2015). These simulations have played crucial roles in understanding the origin of intraplate volcanoes and the evolution of their magma systems.

Obviously, previous geodynamic simulations have demonstrated the likelihood of generating upwelling due to the
85 dehydration of subducted slabs at the deep mantle (Sheng et al., 2016; Li et al., 2019), the piling up and thickening of subducted slabs in the MTZ (Motoki and Ballmer, 2015), and the upward escape of athenospheric material through gaps between slab segments (Liu and Zhou, 2015). However, these simulations possess a degree of universality and do not specifically investigate the mechanism of the Changbaishan volcano. In fact, the three primary mechanisms mentioned above



are intimately linked to the subduction of the Pacific plate. Moreover, the formation of a stagnant Pacific slab in the MTZ is likely significantly influenced by a strong Cenozoic westward mantle flow associated with the Mesozoic subduction of the Izanagi slab, which has not been taken into account in these previous simulations (Sheng et al., 2016; Li et al., 2019; Motoki and Ballmer, 2015; Liu and Zhou, 2015). Consequently, in this paper, we assess the relative significance of the three mechanisms, based on geodynamic reconstruction of the Pacific plate subduction history beneath the CVP since the Cenozoic, as presented by Zhu (2024).

95 **2 Geodynamic model**

In order to explore the origin of the Changbaishan volcano, we use the three-dimensional regional thermochemical geodynamic model based on the results from a global model as inputs, as presented by Zhu (2014), which was determined by best reproducing the structure of the high-speed anomaly zone beneath the CVP. Here we introduce it in brief. This geodynamic model is established using the data assimilation technique (Hu et al., 2016, 2017; Peng et al., 2021a, b) to simulate the subduction history of the Pacific plate since the Cenozoic and uses the outputs of Model 1, the reference model presented by Peng et al. (2021a), at 50 Ma as its initial temperature and viscosity. The thermochemical mantle convection is governed by the equations for the conservation of mass, momentum, and energy, as well as the advection of chemical particles (Hu et al., 2016, 2017; Peng et al., 2021a, b). The discretized model has the mesh resolution of ~46 km in latitude, ~4 – 22 km in longitude and ~16 km within and around the CVP. The resolution in depth is ~7 km near the surface and 10 km between 20 and 710 km, gradually increases to ~35 km at ~1800 km, and maintains this resolution from this depth to the core-mantle boundary. The thermochemical mantle convection is solved using the benchmarked three-dimensional spherical finite element code CitcomS, which was developed by Moresi et al. (1996), Zhong et al. (2000, 2008) and Tan et al. (2006).

The model assimilates time-dependent plate motions and seafloor ages, which are derived from the plate reconstruction of Müller et al. (2016) through the open-source software GPlates (www.gplates.org; Gurnis et al., 2012), over a time interval of 1 Ma. Within this interval, they are interpolated linearly at any given time. The plate motions are imposed on the surface as the top boundary. The seafloor age is employed to determine the thermal structure of the oceanic lithosphere through the half-space cooling model (Turcotte and Schubert, 2014). The surface velocity boundary condition and the upper thermal boundary layer are updated at every time step by using the reconstructed plate motions and seafloor ages. The lithospheric thickness is set to 100 km, which is comparable to that of Northeast China (An and Shi, 2006). The bottom lithospheric temperature is set to the mantle temperature of 1300 °C (e.g., Kumar and Gordon, 2009; Jiménez-Díaz et al., 2012). The boundaries are all slip free at the core-mantle boundary and sidewalls. The core-mantle boundary maintains a fixed temperature of 2500 °C (e.g., Steinberger and Calderwood, 2006; Mao and Zhong, 2018).

The model takes into account chemical compositions. The continental lithosphere is divided into an upper crust, a lower crust and a mantle lithosphere. The oceanic plate is composed of a weak oceanic crust and a chemically buoyant layer. The former is a neutrally buoyant layer, but it has a high viscosity far away (> ~300 km) from a trench while a low viscosity near

the trench ($\leq \sim 300$ km), which causes it act as a lubricating layer and serve a similar function of a sticker layer, decoupling a subducting plate from an overriding plate and producing asymmetric subduction and realistic topography (Cramer et al., 2012). The latter mimics a basaltic crust and possesses a total buoyancy equivalent to that of the Earth's oceanic crust. When it is subducted to a depth of 120 km or greater, its composition transforms into eclogite and its total buoyancy becomes that of the same thick layer with the density of eclogite. An arc-like weak zone is arranged between the continental and oceanic plates to mimic the characteristics of the Earth's subduction zones. This zone aids in decoupling the subducting oceanic plate from the overriding continental plate on both sides of the subduction zone during subduction process.

The model adopts a three-dimensional viscosity which varies with depth, temperature and composition (e.g., Hu et al., 2018; Peng et al., 2021a, b) and satisfies

$$\eta = \eta_0 \cdot C \cdot \exp\left(\frac{E_\eta}{T+T_\eta} - \frac{E_\eta}{T_m+T_\eta}\right), \quad (1)$$

where η is the effective viscosity, η_0 is the depth-dependent background viscosity, C is the compositional multiplier, E_η is the activation energy, T_η is the temperature offset, T is the temperature and T_m is the mantle temperature. The background viscosity η_0 , activation energy E_η and activation temperature T_η vary within four different depth ranges of 0 – 100 km, 100 – 300 km, 300 – 660 km and 660 – 2867 km. For a reference model, the background viscosity of these layers is 10^{20} Pa.s, 10^{20} Pa.s, 10^{21} Pa.s and 3×10^{22} Pa.s, respectively. The activation energy E_η is 25, 42, 25 and 17 kJ/mol, respectively, for the four layers. The temperature offset T_η of these layers is 100, 100, 300 and 300 °C, respectively. Composition affects viscosity by adding a multiplier C , which is a geometric average on for all the compositions within an element, to the pre-exponential factor of viscosity (e.g., Hu et al., 2018; Peng et al., 2021b).

3 Melting in the mantle

In order to estimate the melting in the mantle associated with the subduction of the Pacific slab, we adopt the method used by Vogt et al. (2012). It is assumed, that the degree of both hydrous and dry melting is a linear function of pressure (P) and temperature (T) (e.g., Gerya and Yuen, 2003). For a given pressure and rock composition, the volumetric degree of melting (M_0) is:

$$M_0 = 0 \quad (T < T_{\text{solidus}}) \quad (2)$$

$$M_0 = (T - T_{\text{solidus}})/(T_{\text{liquidus}} - T_{\text{solidus}}) \quad (T_{\text{solidus}} < T < T_{\text{liquidus}}) \quad (3)$$

$$M_0 = 1 \quad (T > T_{\text{liquidus}}) \quad (4)$$

where T_{solidus} and T_{liquidus} are, respectively, solidus and liquidus temperatures, which are related to pressure and calculated through the Equations (5) and (6), as presented by Katz et al. (2003), for a dry mantle.

$$T_{\text{solidus}} = 1085.7 + 132.9P - 5.1P^2 \quad (5)$$

$$T_{\text{liquidus}} = 1780 + 45P - 2P^2 \quad (6)$$

For a wet mantle, if the dissolved water fraction in the melt in weight fraction, $W_{\text{H}_2\text{O}}$, is specified, the calculations of T_{solidus} and T_{liquidus} should be changed into (Katz et al., 2003):

$$T_{\text{solidus}} \rightarrow T_{\text{solidus}} - \Delta T(W_{\text{H}_2\text{O}}) \quad (7)$$

$$T_{\text{liquidus}} \rightarrow T_{\text{liquidus}} - \Delta T(W_{\text{H}_2\text{O}}) \quad (8)$$

155 where $\Delta T(W_{\text{H}_2\text{O}})$ is the temperature decrease in the solidus caused by $W_{\text{H}_2\text{O}}$ and satisfies:

$$\Delta T(W_{\text{H}_2\text{O}}=0) = 0 \quad (9)$$

$$\Delta T(W_{\text{H}_2\text{O}} \geq W_{\text{H}_2\text{O}}^{\text{sat}}) = \Delta T(W_{\text{H}_2\text{O}}^{\text{sat}}) \quad (10)$$

where $W_{\text{H}_2\text{O}}^{\text{sat}}$ is the weight percent of water in a completely saturated melt, which is principally a function of pressure, and satisfies

$$160 \quad \Delta T(W_{\text{H}_2\text{O}}) = K W_{\text{H}_2\text{O}}^\gamma \quad 0 < \gamma < 1 \quad (11)$$

$$W_{\text{H}_2\text{O}}^{\text{sat}} = \chi_1 P^\lambda + \chi_2 P \quad 0 < \lambda < 1 \quad (12)$$

where $K = 43^\circ\text{C wt}\%^{-\gamma}$, $\gamma = 0.75$, $\chi_1 = 12 \text{ wt}\% \text{ GPa}^{-\lambda}$, $\chi_2 = 1 \text{ wt}\% \text{ GPa}^{-1}$ and $\lambda = 0.6$.

4 Results

Zhu (2024) determined the best-fit geodynamic model that can well reproduce the high-speed anomaly zone beneath the
165 CVP. Then he investigated the dynamic subduction process of the Pacific plate since the Cenozoic and presented new
understanding on the origin of the high-speed anomaly zone (Fig. S1 in supporting information). Here we use the best-fit
model to assess the relative significance of the three mechanisms mentioned above.

4.1 Melting due to a combination of upward escape of entrained oceanic asthenosphere material and piling up and thickening of the subducted Pacific slab

170 The preferred geodynamic model presented by Zhu (2024) does not consider the effect of water, but rather focuses on the
upward escape of entrained oceanic asthenosphere material and the piling up and thickening of the subducted Pacific slab in
the MTZ. Therefore, the model can be utilized to estimate the melts in a dry mantle resulting from a combination of these
two mechanisms, and subsequently, assess their roles in the formation of the Changbaishan volcano. Considering that the
Pacific plate started to subduct between 25 and 20 Ma (Zhu, 2024; Mao and Zhong, 2018), so we focus on the dynamic
175 process since 25 Ma.

We use tracers to track the oceanic asthenosphere material flow. As an example, we map the asthenosphere material flow
since 25 Ma in the latitude 41.67°N profile across the CVP (Fig. 2). At 25 Ma, the Pacific plate did not notably subduct (Fig.
2a), but by 20 Ma, the plate had already arrived at the 660-km discontinuity (Fig. 2b). During the period (*i.e.*, between 25
and 20 Ma), about 100-km thick basal asthenosphere was entrained into the MTZ by the subducting Pacific slab, and only a
180 portion (about one third) of these entrained materials could ascend into the mantle wedge through the front of the slab (Fig.

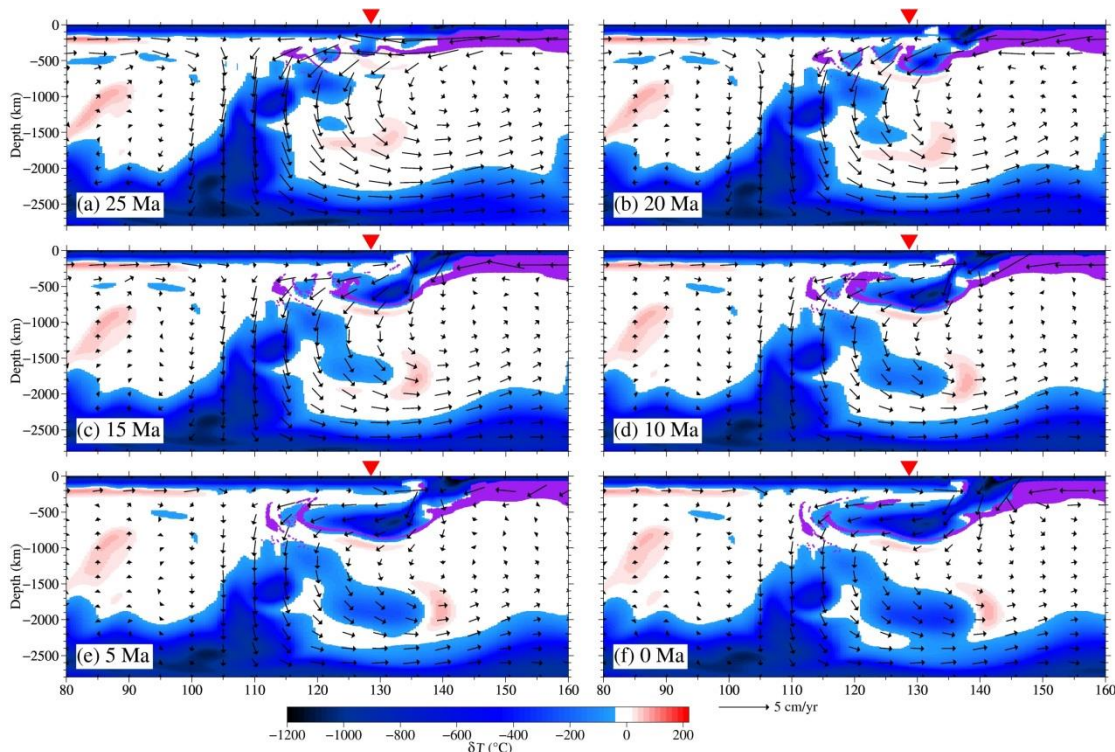


Figure 2: Oceanic asthenosphere material flow (purple) associated with the subduction of the Pacific slab along latitude 41.67°N predicted by the best-fit geodynamic model presented by Zhu (2024). Red triangles stand for the location of the Changbaishan volcano.

185

2b). These ascended materials just piled up beneath or near the CVP and their top depths were shallower than ~300 km at 20 Ma (Fig. 2b). From 20 Ma to the present, more and more asthenospheric material has been entrained into the MTZ, associated with the continuous subduction of the Pacific slab. These materials have moved towards west associated with the westward movement of the Pacific slab and risen up into shallower regions through the front of delaminated lithosphere and the gaps between slabs, and/or between the slab and delaminated lithosphere (Figs. 2c – f). The asthenosphere material located beneath or near the CVP did not reside in the same area but shifted notably. At 20 Ma, the asthenospheric material near a depth of 300 km primarily distributed in the southern margin of the CVP (Fig. S2 in supporting information). By 15 Ma, the material disappeared, while a significant amount of material appeared in the central part of the CVP (Fig. S3 in supporting information). By 10 Ma, the material occurred in the northern margin of the CVP (Fig. S4 in supporting information); and by 5 Ma and the present, there is almost no asthenosphere material beneath or near the CVP (Figs. S5 – S6 in supporting information).

190

195

The piling up and thickening of the subducted Pacific slab primarily occurred between 15 and 10 Ma (Figs. 2c - 2d; Figs. S1e – S1f). The thickening of the slab was mainly caused by the attachment of the delaminated lithosphere to the



subducted Pacific slab. After 10 Ma, the thickening of the slab did not occur notably (Figs. 2e-2f; Figs. S1g – S1h).

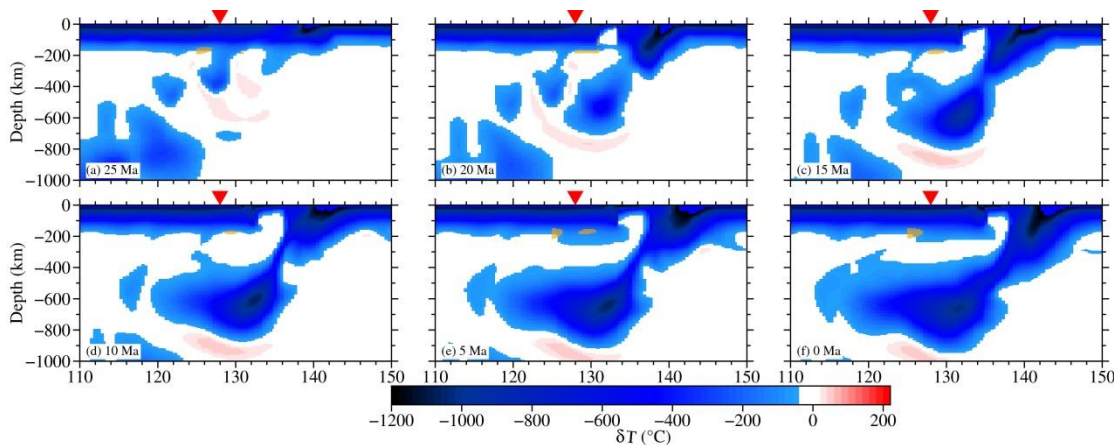
200 Our simulations demonstrate that the oceanic asthenosphere material can be entrained into the MTZ by the subducting Pacific slab and go upwards into mantle wedge through gaps between subducted slabs, supporting many previous simulations (e.g., Liu and Zhou, 2015; Faccenda and Capitanio, 2013) and the conjecture of the upward escape of asthenosphere material inferred from seismic tomography (e.g., Guo et al., 2016, 2018; Tang et al., 2014). However, the upwelling that is caused by a combination of the upward escape of entrained oceanic asthenosphere material with the piling up and thickening of the subducted Pacific slab must lead to the decompression melting of mantle rocks if these two mechanisms are primary. Based on the prediction of our preferred geodynamic model, when $W_{\text{H}_2\text{O}} = 0$, *i.e.*, the mantle is dry, melting does not occur in the mantle beneath the CVP (Figs. S7 – S12 in supporting information). In other words, there is no magma originated from a dry mantle for supporting the volcanism of the Changbaishan volcano, conflicting with the inference that one of the magma chambers of this volcano is located in the mantle (Liu et al., 2015; Fan et al., 2007).
210 Therefore, these two mechanisms are highly unlikely to be the primary causes of the Changbaishan volcano, which does not support the inferences from some seismic tomographic results (e.g., Guo et al., 2016, 2018; Tang et al., 2014), geodynamic simulations (e.g., Liu and Zhou, 2015) and geochemical studies (e.g., Zou et al. 2008).

4.2 Melting due to slab dehydration

Water can be transported to the MTZ by a subducting hydrated oceanic plate, and the mantle overlying the subducted slab can be hydrated through slab dehydration (Sheng et al., 2016; Li et al., 2019). Therefore, we assume that the dehydration of the Pacific slab in the MTZ causes the mantle beneath and near the CVP to become hydrated. We arrange a series of tests with $W_{\text{H}_2\text{O}}$ ranging from 0.0 to 80 wt% to track the $W_{\text{H}_2\text{O}}$ that leads to melting in the mantle beneath and near the CVP since 25 Ma. When $W_{\text{H}_2\text{O}}$ is up to ~20 wt% prior to 10 Ma (Figs. S7-S10 in supporting information) and to ~25 wt% post 10 Ma (Figs. S11-S12 in supporting information), a small amount of melts may occur beneath or near the CVP (Fig. 3). With increasing $W_{\text{H}_2\text{O}}$, the melting area expands and the melting depth gradually deepens. When $W_{\text{H}_2\text{O}} \geq 50$ wt%, the melting depth extends into the MTZ (Figs. S7 - S12 in supporting information). The Changbaishan volcano has a magma source located within the mantle, as suggested by previous investigators (e.g., Liu et al., 2015; Fan et al., 2007). Therefore, based on our findings, it implies the presence of a water-bearing mantle beneath the CVP. The Changbaishan volcano ever erupted at ~15.6 Ma during the Miocene and has primarily erupted since the Pliocene (~5.3 Ma), as reported by Liu et al., 2015. If a portion of the magma from these eruptions originated from the mantle, it would imply that the $W_{\text{H}_2\text{O}}$ must have been no less than 20 wt% during the Miocene (Figs. 3b - 3c; Figs. S8 - S9 in supporting information) and 25 wt% during and after the Pliocene (Figs. 3e – 3f; Figs. S11 – S12 in supporting information). During the Miocene, the melts located just beneath the lithosphere were primarily distributed in the northeast of the CVP (Figs. 4a – 4f). This distribution is consistent with the basalt magma distribution (black areas in Fig. 1b; Liu et al., 2015), suggesting that these melts may have served as the mantle source for the magma that fueled the eruption of the Changbaishan volcano during the Miocene. During and after the
230



Pliocene, the melts were primarily distributed in the northern and southern margins of the CVP and did not fully cover the basalt areas (Figs. 4g – 4l). This suggests that the magma conduit does not extend vertically directly to the craters of the Changbaishan volcano.



235

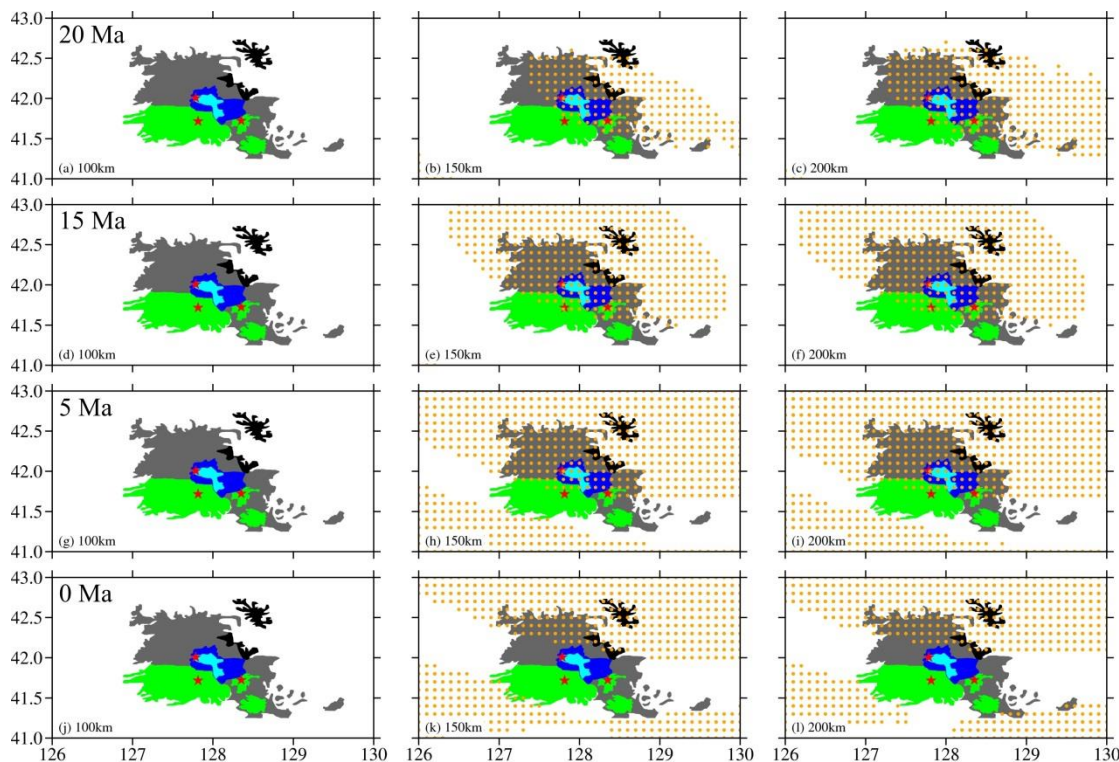
Figure 3: Melts (orange) in the mantle beneath the CVP along latitude 41.67°N at different ages. (a) – (d) $W_{\text{H}_2\text{O}} = 20$ wt%, (e) – (f) $W_{\text{H}_2\text{O}} = 25$ wt%.

5 Discussion

In this paper, we used the geodynamic model that best fits the seismically inferred Pacific slab structure beneath the CVP (Zhu, 2024) to evaluate the relative significance of the three primary conceptual mechanisms mentioned above. The results clearly indicate that the dehydration of the subducted Pacific slab is the primary mechanism controlling the formation of the Changbaishan volcano. The other two mechanisms, namely the upward migration of the entrained oceanic asthenospheric material and the accumulation and thickening of the subducted Pacific slab, play secondary roles. However, if melting occurs in mantle rocks, the water content in the melts, $W_{\text{H}_2\text{O}}$, must be at least 20 - 25 wt% beneath the CVP. Though this value of $W_{\text{H}_2\text{O}}$ is significantly higher than those observed in oceanic basalts and Komatiites (≤ 8 wt%; Gurenko et al., 2016; Sobolev et al., 2016; Shimizu et al., 2001; Dixon et al., 2004) and large igneous provinces (≤ 5.6 wt%; Xia et al., 2016; Wang et al., 2016; Liu et al., 2017), it is comparable to the water contents of the super-hydrous melts found in the lower crust of subduction zonest (≤ 20 wt%; Urann et al., 2022). Therefore, although the Changbaishan volcano is situated in the back-arc region of the western Pacific subduction zone, its magma may originate from the super-hydrous melts within the mantle.

Liu and Zhou (2015) utilized two-dimensional geodynamic models to explore the evolution of oceanic asthenosphere material associated with slab subduction. They discovered that significant amounts of asthenospheric material could be entrained into the deep mantle and speculated that the upwelling caused by the upward episodic escape of entrained

250



255 **Figure 4: Melts (orange) just below the lithosphere beneath and near the CVP at different ages varying with depths.**

asthenospheric material during subduction might account for the enigmatic intraplate volcanism observed at the Changbaishan volcano. However, their geodynamic models did not take into account the subduction of the Izanagi slab into the upper mantle during the Mesozoic, prior to the subduction of the Pacific plate. The subducted Izanagi slab can generate a strong westward mantle flow that plays a vital role in the formation of the long stagnant Pacific slab in the MTZ (Zhu, 2024; Peng et al., 2021a). Our geodynamic model, which does consider the subduction of the Izanagi slab in the Mesozoic, may provide more reasonable predictions and does not support the notion that the upward escape of entrained oceanic asthenosphere material is the primary mechanism of the Changbaishan volcano.

Sheng et al. (2016) and Li et al. (2019) employed two-dimensional thermo-mechanical models to investigate the possible impacts of deep subducted slab dehydration processes and their roles in forming intraplate volcanoes in northeastern China. Their experiments revealed that hydrated subducting slabs can transport water into the MTZ. Subsequently, through slab dehydration, this water hydrates the overlying deep asthenospheric mantle, resulting in the formation of positively buoyant and partially molten hydrous plumes in the hydrated area atop the slabs. These plumes can then propagate upwards and form partially molten mantle regions under the far field continental plate. Consequently, they speculated that the development of



270 the Changbaishan volcano could be correlated with the ascent of these hydrous plumes triggered by stagnant Pacific slab
dehydration in the MTZ. Same as the geodynamic models of Liu and Zhou (2015), those of Sheng et al. (2016) and Li et al.
(2019) did not take into account the subducted Izanagi slab either. However, our geodynamic model predicts that the Pacific
plate could subduct down to the MTZ and move a considerable distance westward. In other words, if the Pacific plate is
hydrated prior to subduction, it will transport water into the MTZ and subsequently dehydrate, forming upward moving
275 hydrous plumes that hydrate the overlying deep asthenospheric mantle. The strong westward mantle flow caused by the
Izanagi slab may weaken the influence of these plumes, but they may still result in high water content in mantle melts. Our
prediction of $W_{\text{H}_2\text{O}} \geq 20 - 25$ wt% aligns with this inference, supporting the notion that the dehydration of the subducted
Pacific slab is the primary mechanism of the Changbaishan volcano (Du and Lei, 2019; Chen et al., 2017; Zhao et al., 2009,
2017; Tian et al., 2016; Wei et al., 2015; Lei et al., 2013; Zhao and Liu, 2010; Tang et al., 2006; Huang and Zhao, 2006; Lei
280 and Zhao, 2005).

6. Conclusion

We explore the origin of the Changbaishan volcano using the geodynamic model with data assimilation that best fits the
structure of the high-speed anomaly zone exceeding 1300 km in the MTZ beneath the CVP. We design a series of
experiments to evaluate the relative importance of three primary conceptual models. The experimental results support that
285 the Changbaishan volcanism primarily originates from the super-hydrous melts in the mantle atop the Pacific slab caused by
the slab dehydration in the MTZ; while the other two mechanisms, the upward escape of the entrained oceanic
asthenospheric material as well as the piling up and thickening of the subducted Pacific slab, may play secondary roles.

Code availability. CitcomS was downloaded from the website of <https://geodynamics.org/resources/citcoms>.

290

Data availability. The raw and final results are available upon reasonable request.

Author contributions. TZ: Conceptualization, formal analysis, numerical computations, funding acquisition, writing original
draft. YG, YX and CD: Formal analysis, review and editing.

295

Competing interests. The contact author has declared that none of the authors has any competing interests.

Acknowledgements

This work was financed by National Natural Science Foundation of China (NSFC Grant No.: 41974103) and a part of the
Self-initiated project, modeling on the geodynamic subduction of the Pacific plate beneath the Changbaishan volcano since



300 the Cenozoic, supported by the Institute of Geophysics, China Earthquake Administration. The numerical calculations in this paper were carried out on the ORISE Supercomputer and the Parallel Computing Platform of Institute of Geophysics, China Earthquake Administration. Most of Figures are generated using Generic Mapping Tools version 6 (Wessel and Smith, 2019).

References

- Acocella, V., Di Lorenzo, R., Newhall, C., and Scandone R.: An overview of recent (1988 to 2014) caldera unrest: Knowledge and perspectives, *Rev. Geophys.*, 53, 896-955, 2015.
- An, M. and Shi, Y.: Lithospheric thickness of the Chinese continent, *Phys. Earth Planet. Inter.*, 159, 257–266, 2006.
- Chen, Y. and Pei, S.: Tomographic structure of East Asia: II. Stagnant slab above 660 km discontinuity and its geodynamic implications, *Earthq. Sci.*, 23, 613-626, 2010.
- Chen, Y., Zhang, Y., Graham, D., Su, S., and Deng, J.: Geochemistry Cenozoic basalts and mantle xenoliths in Northeast China. *Lithos*, 96, 108-126, 2007.
- Choi, H., Choi, S., Schiano, P., Cho, M., Cluzel, N., Devidal, J., and Ha, K.: Geochemistry of olivine-hosted melt inclusions in the Baekdusan (Changbaishan) basalts: Implications for recycling of oceanic crustal materials into the mantle source, *Lithos*, 284-285, 194-206, 2017.
- Cramer, F., Tackley, P., Meilick, I., Gerya, T., and Kaus, B.: A free plate surface and weak oceanic crust produce single-sided subduction on Earth, *Geophys. Res. Lett.*, 39(3), <https://doi.org/10.1029/2011GL050046>, 2012.
- Dixon, J. E., Dixon, T., Bell, D., and Malservisi, R.: Lateral variation in upper mantle viscosity: role of water, *Earth Planet. Sci. Lett.*, 222, 451–467, 2004.
- Du, M. and Lei, J.: Pn anisotropy tomography of Northeast China and its implications to mantle dynamics, *J. Asian Earth Sci.*, 171: 334-347, 2019.
- Faccenda, M. and Capitanio, F.: Seismic anisotropy around subduction zones: Insights from three-dimensional modeling of upper mantle deformation and SKS splitting calculations, *Geochem. Geophys. Geosyst.*, 14: 243-262, 2013.
- Fan, Q., Sui, J., Li, N., Sun, Q., and Xu, Y.: The magmatism and interactive eruption of the two magma chambers in the Tianchi volcano, Changbaishan, *Bull. Mineral. Petrol. Geochem.*, 26(4), 315 – 318, 2007.
- Fan, Q., Z. Zhang. 2012. Study advances in volcanology and chemistry of the Earth's interior during the first decade of the 21st century. *Bull. Mineral. Petrol. Geochem.*, 31(3): 195-204+209 (in Chinese).
- Gerya, T.V., Yuen, D.A., 2003. Characteristics-based marker-in-cell method with conservative finite-differences schemes for modeling geological flows with strongly variable transport properties. *Phys. Earth Planet. Inter.*, 140: 293-318.
- Guo, Z., Y. Chen, J. Ning, Y. Feng, S. Grand, F. Niu, H. Kawakatsu, S. Tanaka, M. Obayashi, J. Ni. 2015. High resolution 3-D crustal structure beneath NE China from joint inversion of ambient noise and receiver functions using NECESSArray data. *Earth Planet. Sci. Lett.*, 416: 1-11.



- Guo, Z., Y. Chen, J. Ning, Y. Yang, J. Afonso, Y. Tang. 2016. Seismic evidence of on-going sublithosphere upper mantle convection for intra-plate volcanism in Northeast China. *Earth Planet. Sci. Lett.*, 433: 31-43.
- Guo, Z., K. Wang, Y. Yang, Y. Tang, Y. Chen, S. Hung. 2018. The origin and mantle dynamics of quaternary intraplate volcanism in Northeast China from joint inversion of surface wave and body wave. *J. Geophys. Res.*, 123: 2410-2425.
- 335 Gurenko, A. A, Kamenetsky, V. S., Kerr, A. C. 2016. Oxygen isotopes and volatile contents of the Gorgona komatiites, Colombia: a confirmation of the deep mantle origin of H₂O. *Earth Planet. Sci. Lett.*, 454: 154–165.
- Gurnis, M., Turner, M., Zahirovic, S., DiCaprio, L., Spasojevic, S., Müller, R. D., Boyden, J., Seton, M., Manea, V. C., Bower, D. J., 2012. Plate tectonic reconstructions with continuously closing plates. *Comput. Geosci.*, 38: 35–42.
- He, C., S. Dong, X. Chen, M. Santosh, S. Niu. 2014. Seismic evidence for plume-induced rifting in the Songliao Basin of
340 Northeast China. *Tectonophys.*, 627: 171-181.
- He, C., M. Santosh. 2016. Seismic tomographic evidence for upwelling mantle plume in NE China. *Phys. Earth Planet. Inter.*, 254: 37-45.
- Hong, H., J. Wu, Q. Wang, K. Li, C. Zhao, Z. Shanguan, Q. Yang, H. Zhang, G. Liu. 2007. Volcanic threat levels and classification of volcanic activity in China. *Seismol. Geol.*, 29(3): 447-458 (In Chinese).
- 345 Hu, J., M. Faccenda, L. Liu. 2017. Subduction-controlled mantle flow and seismic anisotropy in South America. *Earth Planet. Sci. Lett.*, 470: 13-24.
- Hu, J., L. Liu, A. Hermsillo, Q. Zhou. 2016. Simulation of late Cenozoic South American flat-slab subduction using geodynamic models with data assimilation. *Earth Planet. Sci. Lett.*, 438, 1-13.
- Hu, J., L. Liu, Q. Zhou. 2018. Reproducing past subduction and mantle flow using high-resolution global convection models.
350 *Earth Planet. Phys.*, 2: 189-207.
- Huang, J., D. Zhao. 2006. High-resolution mantle tomography of China and surrounding regions. *J. Geophys. Res.*, 111(B09305), doi:10.1029/2005JB004066.
- Jiménez-Díaz, A., J. Ruiz, C. Villaseca, R. Tejero, R. Capote. 2012. The thermal state and strength of the lithosphere in the Spanish Central System and Tajo Basin from crustal heat production and thermal isostasy. *J. Geodyn.*, 58, 29–37.
- 355 Kameyama, M., R. Nishioka. 2012. Generation of ascending flows in the Big Mantle Wedge (BMW) beneath northeast Asia induced by retreat and stagnation of subducted slab. *Geophys. Res. Lett.*, 39(L10309), doi:10.1029/2012GL051678.
- Kumar, R. R., R. G. Gordon. 2009. Horizontal thermal contraction of oceanic lithosphere: The ultimate limit to the rigid plate approximation. *J. Geophys. Res.*, 114 (B01403), doi:10.1029/2007JB005473.
- Lei, J., F. Xie, Q. Fan, M. Santosh. 2013. Seismic imaging of the deep structure under the Chinese volcanos: an overview.
360 *Phys. Earth Planet. Inter.*, 224: 104-123.
- Lei, J., D. Zhao. 2005. P-wave tomography and origin of the Changbai intraplate volcano in Northeast Asia. *Tectonophys.*, 397: 281-295.
- Leonard, T., L. Liu. 2016. The role of a mantle plume in the formation of Yellowstone volcanism. *Geophys. Res. Lett.*, 43: 1132-1139.



- 365 Li, Z., T. Gerya, J. Connolly. 2019. Variability of subducting slab morphologies in the mantle transition zone: Insight from petrological-thermomechanical modeling. *Earth-Sci. Rev.*, 196, <https://doi.org/10.1016/j.earscirev.2019.05.018>.
- Liu, J., S. Chen, Z. Guo, W. Guo, H. He, H. You, H. Kim, G. Sung, H. Kim. 2015. Geological background and geodynamic mechanism of Mt. Changbai volcanoes on the China-Korea border. *Lithos*, 236-237: 46-73.
- Liu, J., Q. Xia, T. Kuritani, E. Hanski, H. Yu. 2017, Mantle hydration and the role of water in the generation of large igneous
370 provinces. *Nature Comm.*, 8: 1824, doi: 10.1038/s41467-017-01940-3.
- Liu, L., Q. Zhou. 2015. Deep recycling of oceanic asthenosphere material during subduction, *Geophys. Res. Lett.*, 42: 2204–2211, doi:10.1002/2015GL063633.
- Lv, Z., H. Hong, H. Wei. 2007. Research on the volcanic earthquake activity mechanism in Changbaishan Tianchi area. *Seismological Res. Northeast China*, 23(1): 40-48 (In Chinese).
- 375 Ma, H., Q. Yang, X. Pan, C. Wu, C. Chen. 2015. Origin of early Pleistocene basaltic lavas in the Erdaobaihe River basin, Changbaishan region. *Acta Petrol. Sin.*, 31(11): 3484 – 3494 (in Chinese).
- Mao, W., Zhong, S. J., 2018. Slab stagnation due to a reduced viscosity layer beneath the MTZ. *Nature Geosci.* 11: 876-881.
- Moresi, L., S. Zhong, M. Gurnis. 1996. The accuracy of finite element solutions of Stokes's flow with strongly varying viscosity. *Phys. Earth Planet. Inter.*, 97: 83–94.
- 380 Motoki, M., M. Ballmer. 2015. Intraplate volcanism due to convective instability of stagnant slabs in the MTZ. *Geochem. Geophys. Geosyst.*, 16: 538-551.
- Müller, R. D., M. Seton, S. Zahirovic, S. E. Williams, K. J. Matthews, N. M. Wright, G. E. Shephard, K. T. Maloney, N. Barnett-Moore, M. Hosseinpour, D. J. Bower, J. Cannon. 2016. Ocean basin evolution and global-scale plate reorganization events since pangea breakup. *Annu. Rev. Earth Planet. Sci.*, 44: 107-138.
- 385 Peng, D., L. Liu, J. Hu, S. Li, M. Liu. 2021a. Formation of east Asian stagnant slabs due to a pressure-driven Cenozoic mantle wind following Mesozoic subduction. *Geophys. Res. Lett.*, 48(18), e2021GL094638, <https://doi.org/10.1029/2021GL094638>.
- Peng, D., L. Liu, Y. Wang. 2021b. A newly discovered Late-Cretaceous East Asian flat slab explains its unique lithospheric structure and tectonics. *J. Geophys. Res.*, 126(10), e2021JB022103.
- 390 Sheng, J., J. Liao, T. Gerya. 2016. Numerical modeling of deep oceanic slab dehydration: implications for the possible origin of far field intra-continental volcanoes in northeastern China. *J. Asian Earth Sci.*, 117: 328-336.
- Shimizu, K., Komiya, T., Hirose, K., Shimizu, N., Maruyama, S. Cr-spinel. 2001. An excellent micro-container for retaining primitive melts-implications for a hydrous plume origin for komatiites. *Earth Planet. Sci. Lett.*, 189: 177–188.
- Sobolev, A. V., E. Asafov, A. Gurenko, N. Arndt, V. Batanova, M. Portnyagin, D. Garbe-Schönberg, S. Krashenninikov.
395 2016. Komatiites reveal a hydrous Archaean deep-mantle reservoir. *Nature*, 531: 628–632.
- Steinberger, B., A. R. Calderwood. 2006. Models of large-scale viscous flow in the Earth's mantle with constraints from mineral physics and surface observations. *Geophys. J. Int.*, 167: 1461–1481.



- Strak, V., W. Schellart. 2014. Evolution of 3-D subduction-induced mantle flow around lateral slab edges in analogue models of free subduction analysed by stereoscopic particle image velocimetry technique. *Earth Planet. Sci. Lett.*, 403: 368 - 379.
- Takeuchi, N., H. Kawakatsu, S. Tanaka, M. Obayashi, Y. Chen, J. Ning, S. Grand, F. Niu, J. Ni, R. Iritani, K. Idehara, T. Tonegawa. 2014. Upper mantle tomography in the Northwestern Pacific region using triplicated P waves. *J. Geophys. Res.*, 119: 7667-7685.
- Tan, E., E. Choi, P. Thoutireddy, M. Gurnis, M. Aivazis. 2006. GeoFramework: Coupling multiple models of mantle convection within a computational framework. *Geochem. Geophys. Geosyst.*, 7(Q06001), doi:10.1029/2005GC001155.
- Tang, J., G. Zhao, J. Wang, Y. Zhan, Q. Deng, X. Chen. 2006. Study of the formation mechanism for volcanism in Northeast China based on deep electric structure. *Acta Petrologica Sinica*, 22(6): 1503-1510 (in Chinese).
- Tang, Y., M. Obayashi, F. Niu, S. Grand, Y. Chen, H. Kawakatsu, S. Tanaka, J. Ning, J. Ni. 2014. Changbaishan volcanism in northeast China linked to subduction-induced mantle upwelling. *Nature Geosci.*, 7: 470-475.
- Tatsumi, Y., S. Maruyama, S. Nohda. 1990. Mechanism of backarc opening in the Japan Sea: role of asthenospheric injection. *Tectonophys.*, 181: 299-306.
- Thybo, H., E. Perchuc. 1997. The seismic 8° discontinuity and partial melting in continental mantle. *Science*, 275(5306): 1626-1629.
- Tian Y, H. Zhu, D. Zhao, C. Liu, X. Feng, T. Liu, J. Ma. 2016. MTZ structure beneath the Changbai volcano: Insight into deep slab dehydration and hot upwelling near the 410 km discontinuity. *J. Geophys. Res.*, 121: 5794-5808.
- Turcotte, D., G. Schubert. 2014. *Geodynamics* (Third edition). Cambridge University Press, p. 189-193.
- Urann, B. M., V. Le Roux, O. Jagoutz, O. Müntener, M. D. Behn, E. J. Chin. 2022. High water content of arc magmas recorded in cumulates from subduction zone lower crust. *Nature Geosci.*, 15: 501-508.
- Vogt, K., T. Gerya, A. Castro. 2012. Crustal growth at active continental margins: Numerical modeling. *Phys. Earth Planet. Inter.*, 192-193: 1-20.
- Wang, F., W. Chen, Z. Peng. 2000. Features of excess of U in volcanic rocks of Changbaishan Tianchi: The evidence for subduction of western Pacific plate. *Seismol. Geol.*, 22(Suppl): 87-94 (in Chinese).
- Wang, X., S. Wilde, C. Pang. 2016. Origin of arc-like continental basalts. Implications for deep-Earth fluid cycling and tectonic discrimination. *Lithos*, 261: 5-45.
- Wei, H., G. Liu, J. Gill. 2013. Review of eruptive activity at Tianchi volcano, Changbaishan, northeast China: Implications for possible future eruptions. *Bull. Volcano.*, 75(4): 1-14.
- Wei, W., J. Xu, D. Zhao, Y. Shi. 2012. East Asia mantle tomography: New insight into plate subduction and intraplate volcanism. *J. Asian Earth Sci.*, 60: 88-103.
- Wei, W., D. Zhao, J. Xu, F. Wei, G. Liu. 2015. P and S wave tomography and anisotropy in Northwest Pacific and East Asia: Constraints on stagnant slab and intraplate volcanism. *J. Geophys. Res.*, 120: 1642-1666.



- Wu, J., Y. Ming, H. Zhang, G. Liu, L. Fang, W. Su, W. Wang. 2007. Earthquake swarm activity in Changbaishan Tianchi volcano. *Chin. J. Geophys.*, 50(4): 1089 – 1096 (In Chinese).
- Wang, Y., C. Li, H. Chen. 1999. Tectonic setting of Cenozoic volcanism in Northeastern China. *Geological Rev.*, 45(s1): 180-189 (In Chinese).
- 435 Xia, Q., Y. Bi, P. Li, W. Tian, X. Wei, H. Chen. 2016. High water content in primitive continental flood basalts. *Sci. Rep.*, 6, 25416.
- Xu, J., G. Liu, J. Wu, Y. Ming, Q. Wang, D. Cui, Z. Shangguan, B. Pan, X. Lin, J. Liu. 2012. Recent unrest of Changbaishan volcano, northeast China: A precursor of a future eruption? *Geophys. Res. Lett.*, 39(L16305), doi:10.1029/2012GL052600.
- Zhao, D., Y. Isozaki, S. Maruyama. 2017. Seismic imaging of the Asian orogens and subduction zones. *J. Asian Earth Sci.*,
440 145: 349-367.
- Zhao, D., L. Liu. 2010. Deep structure and origin of active volcanoes in China. *Geosci. Front.*, 1: 31-44.
- Zhao, D., Y. Tian, J. Lei, L. Liu, S. Zheng. 2009. Seismic image and origin of the Changbai intraplate volcano in East Asia: Role of big mantle wedge above the stagnant Pacific slab. *Phys. Earth Planet. Inter.*, 173: 197-206.
- Zhong, S., A. McNamara, E. Tan, L. Moresi, M. Gurnis. 2008. A benchmark study on mantle convection in a 3-D spherical
445 shell using CitcomS. *Geochem. Geophys. Geosyst.*, 9(Q10017), doi:10.1029/2008GC002048.
- Zhong, S., M. Zuber, L. Moresi, M. Gurnis. 2000. Role of temperature-dependent viscosity and surface plates in spherical shell models of mantle convection. *J. Geophys. Res.*, 105(11): 11063 - 11082.
- Zhu, T. 2024. Origin of high-speed anomaly zone beneath the Changbaishan volcanic province in Northeast Asia: insights from simulation of the Cenozoic Pacific plate subduction using geodynamic models with data assimilation. *J. Asian Earth
450 Sci.*, submitted.
- Zou, H., Q. Fan, Y. Yao. 2008. U–Th systematics of dispersed young volcanoes in NE China: asthenosphere upwelling caused by piling up and upward thickening of stagnant Pacific slab. *Chemical Geology*, 255: 134–142.
- Zou, H., Q. Fan, Q. Zhang. 2010. Rapid development of the great Millennium eruption of Changbaishan (Tianchi) Volcano, China/North Korea: Evidence from U–Th zircon dating. *Lithos*, 119(3-4): 289-296.